Interface Wavelength Between Supersonic Jets and Subsonic Flowfields

Lawrence J. De Chant*
Texas A&M University, College Station, Texas 77843
Jonathan A. Seidel†
NASA Lewis Research Center, Cleveland, Ohio 44135
and
Malcolm J. Andrews‡
Texas A&M University, College Station, Texas 77843

Nomenclature

f = streamwise varying function for separation of variables
g = cross-stream varying function for separation of variables
M = Mach number
p = static pressure
r = radial coordinate
s = strained coordinate
U = freestream velocity
x = streamwise coordinate
β = $|M^2 - 1|^{1/2}$
λ = eigenvalue
ξ = interface function
ϕ = velocity potential

Subscripts

c = critical (first minimum) location
eff = effective value
m = maximum value
s = slipline location
0 = total condition or perturbation level
1 = supersonic primary stream or perturbation level
2 = subsonic secondary stream or perturbation level

Introduction

SUPERSONIC ejector nozzles are currently of considerable interest for aeropropulsion applications because of their noise suppression and improved performance capabilities.[1] An important limiting form of the ejector flow is represented by a freejet effluxing into an infinite coflowing stream. Thus, the structure of the plume or jet issuing from the main nozzle is of considerable interest to flight system designers.

The problem is axisymmetric with an unconfined, supersonic primary stream and a subsonic secondary stream shear layer. Early solutions for freejet flows were developed by Prandtl[2] and later by Pai[3] based upon perturbations about inlet quantities. An improvement was made by Pack,[4] who used a perturbation about the velocity field at the slipline (vortex sheet).

Here, a modification to the streamline perturbation model of Pack is derived using a strained coordinate technique that extends the range of application to larger pressure ratios for jet flows. A comparison is performed to evaluate the strained coordinate solution for available large-pressure ratio-freejet experiments.

Pack[4] developed a linear analysis for freejets using a perturbation about the slipline. For axisymmetric flows the slipline displacement critical location (first minimum) x_c is[4]

$$x_c/2 = 1.22\beta_{1s} \tag{1}$$

Equation (1) is limited to relatively small pressure ratios between streams. Moreover, Pack's solution admits the trivial solution of $\phi_1(x, r) = \xi(x) = 0$ for $p_1 = p_2$, which is not experimentally or analytically valid,[5] where ξ describes the slipline displacement.

Analysis

To overcome the pressure ratio restrictions and singularity for $p_1 = p_2$ in Pack's streamline perturbation analysis, a strained coordinate slipline perturbation method has been formulated. A full description of the strained coordinate method may be found in Refs. 6 and 7. Motivation for the use of the strained coordinates comes from the recognition that Pack's analysis fails for large-pressure ratios between streams associated with large displacement of the interface. Defining new coordinates that better approximate the location of the slipline velocity boundary condition might be expected to give a better solution.

The strained coordinate method starts by considering the solution of ordinary differential equations resulting from a separation of the variable solution of the governing small disturbance wave equation[8] with $\phi(x, r) = f(x)g(r)$ without invoking a boundary condition transfer[6] approximation:

$$\frac{d^2 f}{dx^2} + \left(\frac{\lambda_n}{\beta_{1s}}\right)^2 \frac{1}{[1 + \xi(x)]^2} f = 0 \tag{2}$$

where $J_0(\lambda_n) = 0$ and $n = 1, 2, 3, \ldots$. The slipline displacement is approximated as

$$\xi(x) \approx \xi_m \sin^2(\lambda_n x/2\beta_{1s}) \qquad \xi_m \equiv \beta_{1s}^2 \varepsilon \equiv \beta_{1s}^2[1 - (U_1/U_{1s})] \tag{3}$$

Since Pack's solution is singular for zero displacement, $\xi = 0$, a stretching transformation for the displacement is introduced with the displacement magnitude ξ_m as the appropriate perturbation parameter. New (strained) coordinates are introduced as

$$x = s + x_2(s)\xi_m^{\frac{1}{2}} + \cdots \tag{4}$$

where s is the new coordinate and $x_2(s)$ is to be determined. Similarly, the basic solution is perturbed as

$$f = f_0 + \xi_m^{\frac{1}{2}} f_1 + \cdots \tag{5}$$

The expansions defined by Eqs. (4) and (5) and their transformed derivatives are substituted into Eq. (2) to yield a system of equations for $f_0(s)$ and $f_1(s)$. The $\mathcal{O}(1)$ equation yields the expected simple harmonic equation as Eq. (2) with $\xi(x) = 0$ and to $\mathcal{O}(\xi_m^{1/2})$:

$$\frac{d^2 f_1}{ds^2} + \left(\frac{\lambda_n}{\beta_{1s}}\right)^2 f_1 = x_2'' \frac{d\dot{f}_0}{ds} + 2x_2' \frac{d^2 f_0}{ds^2} + 2\sin^2\left(\frac{\lambda_n s}{2\beta_{1s}}\right)\left(\frac{\lambda_n}{\beta_{1s}}\right)^2 f_0 \tag{6}$$

To prevent the existence of solutions that grow unphysically large, $x_2(s)$ is chosen so that it approximately eliminates the right-hand side of Eq. (6). This can be considered as eliminating a forcing term in a harmonic system.[6] One choice to approximately remove the right-hand side of Eq. (6) is to set $x_2(s) = s/2$; then $x_2'' = 0$, and the strained coordinate s is given by

$$s = \frac{x}{\left(1 + \frac{1}{2}\xi_m^{\frac{1}{2}}\right)} \tag{7}$$

Following Lighthill,[7] since the $\mathcal{O}(1)$ solution of Eq. (2) is the same as the unstrained problem (except $x = s$), Eq. (7) is introduced into the solution for the unstrained problem, Eq. (1). Since Eq. (7) involves straining by a constant, Eq. (1) may be simply modified by substitution of the strained coordinate. Additionally, since the current formulation is valid for small pressure ratios because of the stretching transformation of Eq. (4), the strained coordinate solutions are modified using the particular solution referenced by Love

Received Feb. 11, 1995; revision received Jan. 2, 1996; accepted for publication Feb. 16, 1996.

*Graduate Research Assistant, Department of Mechanical Engineering, MS 3123, Box 172.
†Aerospace Engineer, HSR Propulsion Systems Studies Project Office, MS AAC-1, 21000 Brookpark Road.
‡Assistant Professor, Department of Mechanical Engineering, MS 3123, Box 172. Member AIAA.

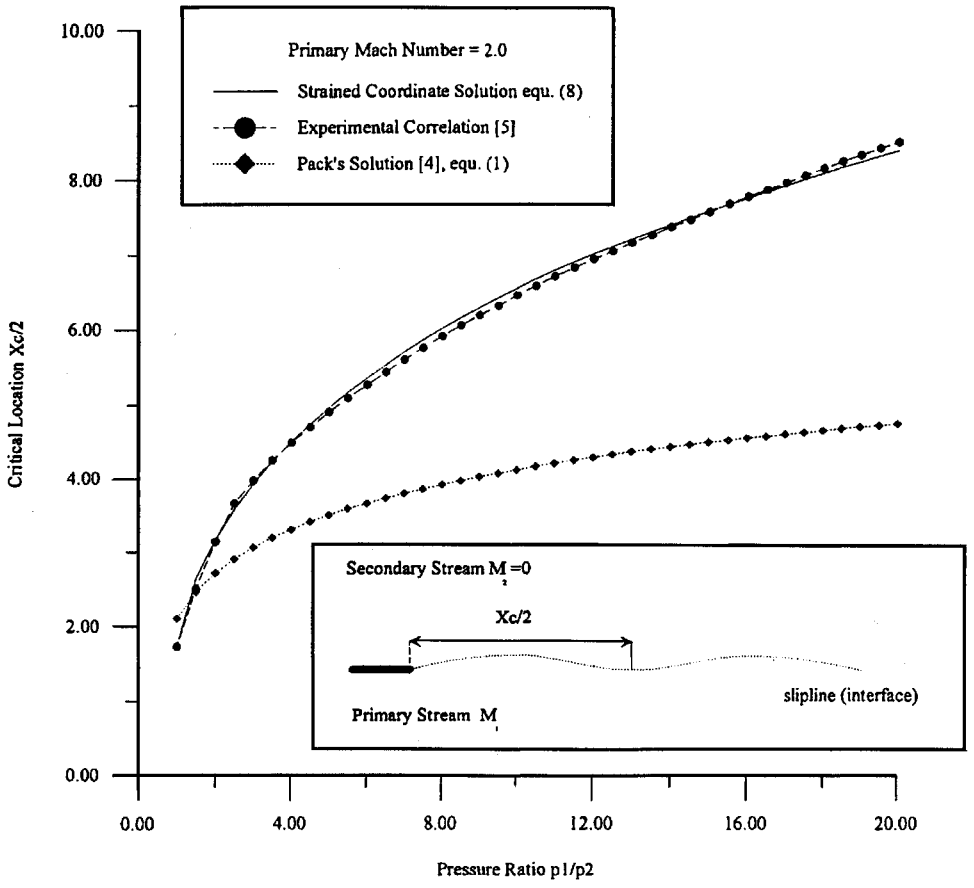

Fig. 1 Axisymmetric jet critical location vs pressure ratio for primary Mach numbers $M_1 = 2.0$ as predicted by strained coordinate solution, Eq. (8), and Pack's solution, Eq. (1), with comparison to the empirical correlation of Love et al.[5]

Table 1 Comparison of strained coordinate model [Eq. (8)] with empirical correlations of Love et al.[5]

Primary Mach number ($p_1/p_2 = 1.0$–20.0)	RMS error, %, $\text{err}_{\text{RMS}} = [1/N \sum e_{i,\text{rel}}^2]^{1/2}$, $N = 20$	Maximum relative error, %
1.2	6.34	9.48
2.0	1.15	5.44
3.0	4.12	5.19
4.0	9.03	10.10

et al.[5] that is valid for pressure ratios precisely equal to 1. Thus, the solutions may be written as follows:

Axisymmetric:

$$x_c/2 = 1.22\beta_{\text{eff}} - 0.22\beta_{1s} \equiv 1.22\left(1 + \tfrac{1}{2}\xi_m^{\frac{1}{2}}\right)\beta_{1s} - 0.22\beta_{1s} \quad (8)$$

and by analogy with Eq. (8), the two-dimensional solution is

$$x_c/2 = 2\beta_{\text{eff}} - \beta_{1s} \equiv 2\left(1 + \tfrac{1}{2}\xi_m^{\frac{1}{2}}\right)\beta_{1s} - \beta_{1s} \quad (9)$$

Equations (8) and (9) are the final strained coordinate solutions for the first minimum critical slipline location.

Comparison with Experiments

Figure 1 compares the strained coordinate solution, Eq. (8), with the axisymmetric, freejet experiment of Love et al.[5] for several primary Mach numbers, as well as with Pack's solution, Eq. (1). Figure 1 shows that the comparison between the strained coordinate solution and the experimental data is reasonable and also a considerable improvement over Pack's solution. Defining a relative rms error between the method and the experimental correlation yields the results presented in Table 1 for a pressure ratio range of $p_1/p_2 = 1.0$–20.0. Table 1 shows that the strained coordinate solution provides a good prediction of freejet critical locations over a full range of Mach numbers and pressure ratios.

Conclusions

A linearized, potential flow solution for freejet, axisymmetric, and two-dimensional flows has been developed based upon a strained coordinate extension to Pack's slipline perturbation solution. The slipline is described by the streamwise location of the first minimum of slipline displacement. Freejet experimental data were used to check this solution and also to compare with other classical relationships. The strained coordinate model provides good overall results for a large range of Mach numbers (1.2–4.0) and stream pressure ratios (1.0–20.0).

Note that the confining effects of the ejector flow are contained within the basic small disturbance equation expansion terms, $\beta_{1s} = |M_{1s}^2 - 1|^{1/2}$, and so the strained coordinated solutions, Eqs. (8) and (9), are directly applicable to supersonic ejector flows. The closed-form result is useful for a number of applications including preliminary design problems for which a computational fluid dynamics simulation is inappropriate.

Acknowledgments

Partial support for this work was provided under NASA Grant NAG-1512, John K. Lytle, technical representative, and from the NASA Graduate Student Researchers Program. Thanks also to Jerald A. Caton, Texas A&M University, for his continued support and encouragement.

References

[1]Champagne, G. A., "Jet Noise Reduction Concepts for the Supersonic Transport," AIAA Paper 91-3328, Sept. 1991.

[2]Prandtl, L., "Ueber die stationaeren Wellen in einem Gasstrahle," *Physik Z*, Vol. 5, 1904, pp. 599–601.

[3]Pai, S. I., "On Two-Dimensional Supersonic Flow of a Jet in Uniform Stream," *Journal of the Aeronautical Sciences*, Vol. 19, No. 1, 1952, pp. 61–65.

[4]Pack, D. C., "A Note on Prandtl's Formula for the Wavelength of a Supersonic Gas Jet," *Quarterly Journal of Mechanics and Applied Mathematics*, Vol. 3, Pt. 2, 1950, pp. 173–181.

[5]Love, E. S., Grigsby, C. E., Lee, L. P., and Woodling, M. J., "Experimental and Theoretical Studies of Axisymmetric FreeJets," NASA TR R-6, 1959.

[6]Nayfeh, A., *Perturbation Methods*, Wiley, New York, 1973, pp. 57–109.

[7]Lighthill, M. J., "A Technique for Reducing Approximate Solutions to Physical Problems Uniformly Valid," *Zeitschrift für Flugwissenschaften*, Vol. 9, 1961, pp. 267–275.

[8]Anderson, J. D., *Modern Compressible Flow*, McGraw–Hill, New York, 1982.

Sound Generation by a Ring Vortex–Shock Wave Interaction

A. P. Szumowski* and G. B. Sobieraj†
Warsaw University of Technology, 00-665 Warsaw, Poland

Introduction

FLOWS with supercritical speeds, which are characterized by shock waves, are often accompanied by vortices of various intensities. Both structures may interact, leading to impulsive noise radiation. This phenomenon is observed in numerous external and internal transonic flows. In the case of helicopter or cascade blades operating at high-subsonic-flow Mach numbers, a shock that appears on the low-pressure blade surface may interact with the vortex street from preceding blades. Similarly, in an underexpanded jet, the vortices at the shear layer periodically pass through the shock-wave pattern of the jet, causing intensive noise.[1]

These aerodynamic problems have motivated many investigators to elucidate the physics of the shock–vortex interaction process. Theoretical and experimental investigations have been done. In the theoretical studies, analytical[2,3] and numerical methods[4–6] were considered, and have been used to predict both the sound wave formed at the region of interaction and the shock-wave deformation when it passes through the vortex.

The theoretical investigations of the interaction process were performed for a cylindrical vortex and a plane-incident shock wave. This case also was examined experimentally by Dosanjh and Weeks[7] and Naumann and Hermans,[8] who used a starting vortex shed from the trailing edge of the airfoil when the shock wave passes over it. The main result of both the theoretical and the experimental studies is the finding that the two-dimensional vortex–shock wave interaction produces a quasicylindrical sound wave (Fig. 1) of nonuniform strength; the strength of the sound wave decreases along its front with increasing distance from the triple point A. However, to some extent a different wave pattern can be expected when the ring vortex–shock wave interaction appears in an axisymmetric flow. Also, when the flow in a jet occurs along the axes of the ring vortex, it can influence the sound-wave configuration. This problem is studied in the present paper for the head vortex of a starting jet.

Apparatus

A conventional shock tube, internal diameter $D = 50$ mm, was used in the experiments. A starting jet was incident on a perpendicular wall placed at a distance of two tube diameters from the shock-tube exit. The free jet was visualized by means of a schlieren system in which a spark source of flash duration about 1 μs was used for a illumination. The shock-wave Mach number in the shock tube was determined by measuring the time traveled by the shock wave over a test distance of 100 mm.

Results

A set of photographs (Fig. 2) shows the successive phases of the vortex–shock wave interaction process for the jet-flow Mach number $M = 0.65$ (the jet-flow Mach number was calculated on the basis of the shock-wave Mach number). The first photograph shows a bow shock wave reflected at the wall and a head vortex just before interaction. The central part of the shock wave moves slowly because of the opposite flow caused by the jet (photograph 2). Because of this effect, the shock wave loses its previous shape, which is analogous to the two-dimensional flow case.[8] However, in contrast to the two-dimensional case, the shock deformation is now much stronger owing to the high velocity of the jet flow. In the stage shown in photograph 4, three shock-wave elements can be distinguished: 1) a nearly normal shock wave in the vortex plane moving slowly upstream; 2) an undisturbed bow shock wave outside

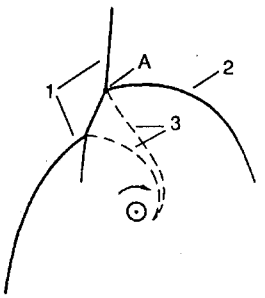

Fig. 1 Wave pattern for a cylindrical vortex–plane shock wave interaction (from Ref. 8): 1) shock front, 2) sound wave, 3) contact surface, and A) triple point.

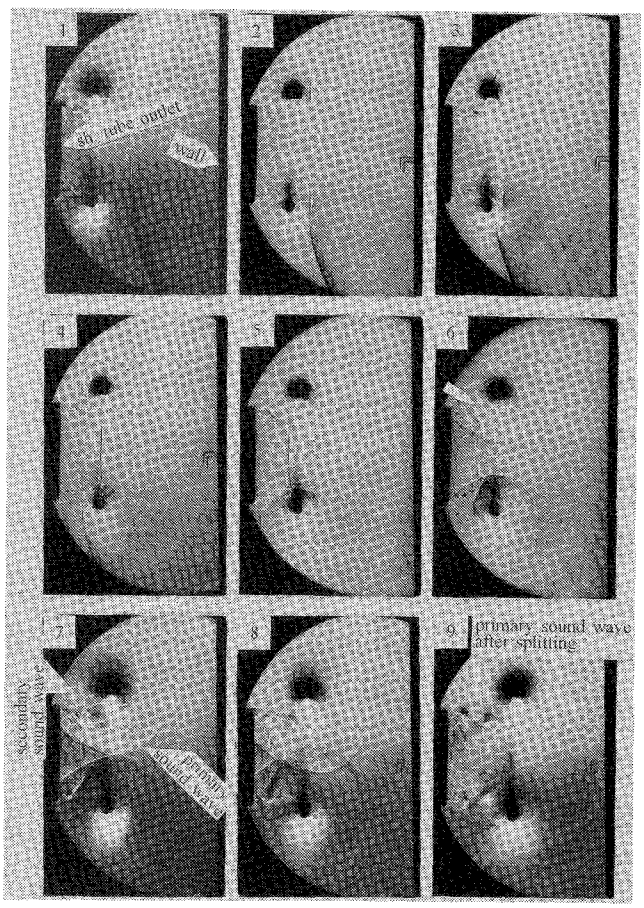

Fig. 2 Schlieren photographs showing the transient flow patterns during the ring vortex–shock wave interaction. Delay time (ms) in relation to the moment when the shock wave leaves the tube: 1) 0.56, 2) 0.59, 3) 0.615, 4) 0.65, 5) 0.69, 6) 0.71, 7) 0.76, 8) 0.8, and 9) 0.95.

Received July 18, 1995; revision received Sept. 29, 1995; accepted for publication Oct. 6, 1995.

*Professor, Department of Aerodynamics, ul. Nowowiejska 24.

†Senior Research Scientist, Department of Aerodynamics, ul. Nowowiejska 24.